

- (23) D. R. Miller and C. W. Macosko, *Macromolecules*, **13**, 1063 (1980); (b) K. Dusek, M. Ilavsky, and S. Lunak, *J. Polym. Sci., Polym. Symp.*, No. 53, 29 (1975).  
 (24) G. Hagnauer, unpublished results.

- (25) **Note Added in Proof:** Compositions estimated in Table III were based on  $\lambda_{\max}$  values close to those of model compounds, namely 420, 445, 460, and 470 nm for species 2', 3', 4', and 5', respectively.

## Block Copolymers near the Microphase Separation Transition. 2. Linear Dynamic Mechanical Properties

Frank S. Bates\*

AT&T Bell Laboratories, Murray Hill, New Jersey 07974. Received April 27, 1984

**ABSTRACT:** Three 1,4-polybutadiene-1,2-polybutadiene diblock copolymers near the microphase separation transition (MST) have been examined rheologically. The low-frequency linear dynamic shear moduli are shown to be strongly dependent on the phase state of these samples, which exhibit an upper critical temperature. Heating a microphase-separated (ordered) sample containing 38% 1,4-polybutadiene through the MST produces a discontinuity in both the elastic modulus and dynamic viscosity at a temperature  $T_m$ , corresponding to the first-order melt transition from the ordered to the disordered (homogeneous) state. Cooling from the disordered state produces no discontinuity in the moduli at  $T_m$ ; instead, the polymer melt exhibits metastable behavior down to the stability limit in temperature,  $T_s < T_m$ . Below  $T_s$ , the viscoelastic response is characteristic of microphase-separated block copolymer, regardless of thermal history. These findings quantitatively verify the predicted phase behavior for diblock copolymers characterized by an upper critical temperature.

### Introduction

Over the past several decades, researchers have reported extensively on the viscoelastic properties of block copolymers. Yet, with few exceptions, these investigations have dealt exclusively with microphase-separated systems. As a result, the rheological properties of block copolymers near the microphase separation transition (MST) are not well understood. This situation is a natural consequence of the difficulty of preparing bulk block copolymers near the phase boundary. As demonstrated by Leibler,<sup>1</sup> the critical point in a block copolymer phase diagram scales as  $(\chi N)_c = 10.5$ , where  $N$  is the degree of polymerization and  $\chi$  is the Flory segment-segment interaction parameter. This prediction is based upon an upper critical temperature, often referred to as an upper critical solution temperature (UCST), for which  $\chi > 0$ . Therefore, the MST can be approached from the microphase-separated (ordered) state by decreasing either  $\chi$  or  $N$ . In practice,  $N$  must be adjusted so as to bring  $\chi N$  close to the phase boundary; varying temperature ( $\chi \sim T^{-1}$ ) then provides the means of probing the sample rheology through the MST. Since most polymer pairs are characterized by a relatively large interaction parameter, high molecular weight diblock copolymers ( $N > 100$ ) near the critical point are correspondingly rare. Until present, the rheology of block copolymers near the MST has been studied in only a few samples.<sup>2-4</sup>

Chung et al.<sup>2</sup> and Gouinlock and Porter<sup>3</sup> have both examined the dynamic mechanical properties of a styrene-butadiene-styrene triblock copolymer (7S-43B-7S) at elevated temperatures and have reported similar results. These authors found that upon raising the temperature, the low-frequency dynamic elastic modulus and dynamic viscosity decreased dramatically between 140 and 150 °C. Above this transition temperature the rheological behavior was Newtonian, while below 140 °C it was highly non-Newtonian. Both groups related these findings to the block copolymer microphase separation transition. Widmaier and Meyer<sup>4</sup> subsequently examined the rheological

**Table I**  
Molecular Characterization

sample	$N_n \times 10^{-2}$ <sup>a</sup>	$N_w/N_n$ <sup>b</sup>	$\Phi$ <sup>c</sup>
BB2	10.6	1.03	0.46
BB6	13.3	1.05	0.38
BB7	15.5	1.05	0.48

<sup>a</sup> Number-average degree of polymerization. <sup>b</sup> Polydispersity index as determined by high-pressure size exclusion chromatography. <sup>c</sup>  $\Phi = N_{1,4}/(N_{1,4} + N_{1,2})$  as determined by <sup>13</sup>C NMR.

properties of a styrene-isoprene-styrene triblock copolymer (14S-17I-14S) and concluded that a structural transition occurred in that sample at 225 °C.

In the first of this series of articles,<sup>5</sup> we reported on the preparation and physical characterization of a model set of 1,4-polybutadiene-1,2-polybutadiene diblock copolymers near the MST. In that report, the phase state of the polymers was identified by qualitatively examining the flow behavior of each sample. In another recent article,<sup>6a</sup> the structure of the homogeneous melt state was determined by small-angle neutron scattering (SANS); this provided a direct measurement of the segment-segment interaction parameter, which determines the location of the MST. The present text describes the quantitative linear dynamic mechanical analysis of three of these diblock copolymers, lying near the phase boundary. These results, while consistent with those described above, further provide a detailed description of the thermodynamic behavior of block copolymers near the microphase separation (order-to-disorder) transition, including the identification of the equilibrium and stability limits between the microphase-separated and homogeneous melt states. These findings, together with the SANS results, quantitatively confirm the mean-field predictions of Leibler<sup>1</sup> concerning the microphase separation transition in diblock copolymers.

### Experimental Section

Synthesis and characterization of the diblock copolymers have been previously reported.<sup>5</sup> Characterization data for the three presently discussed samples are listed in Table I. The 1,4-polybutadiene block microstructure is 89% 1,4 (cis and trans) and 11% 1,2, while that of the 1,2-polybutadiene block is >98% 1,2.

\* Present address: Department of Chemical Engineering, California Institute of Technology, Pasadena, CA 91125.

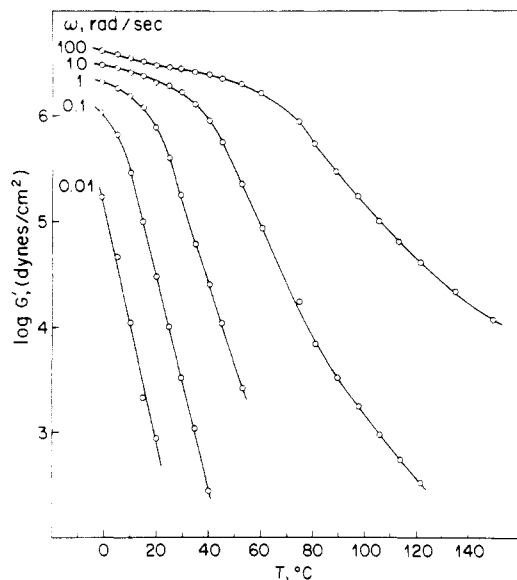


**Figure 1.** Dynamic elastic modulus of sample BB2, a homogeneous diblock copolymer.

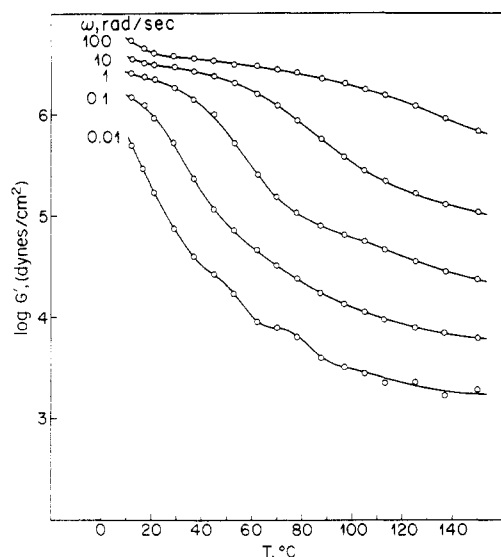


**Figure 2.** Dynamic elastic modulus of sample BB7, a microphase-separated diblock copolymer.

Dynamic shear moduli were determined with a Rheometrics dynamic spectrometer (RDS-7700) in an oscillating parallel-plate mode between  $-5$  and  $+150$  °C and from  $0.01$  to  $100$  rad/s in frequency. Sample geometry was established with  $5$ -cm-diameter platens, at a gap of  $2$ – $3$  mm, which was corrected for apparatus thermal expansion. Polymer samples were stored and mounted onto the platen in a high-purity argon glovebox, and the temperature-controlled sample chamber was purged with nitrogen during sample measurement. Measurements were performed in the linear viscoelastic regime with a maximum shear strain amplitude of  $0.15$ . All data were taken above the glass transition region of the polybutadiene samples.

## Results

The viscoelastic parameters employed in characterizing the properties of block copolymers near the MST derive from the complex shear modulus

$$G^* = G' + iG''$$

where  $G'$  represents the in-phase or elastic component and  $G''$  the out-of-phase or dissipative component of  $G^*$ .  $\eta'$ , the dynamic viscosity, is related to  $G''$  through the frequency  $\omega$ :

$$\eta' = G''/\omega$$

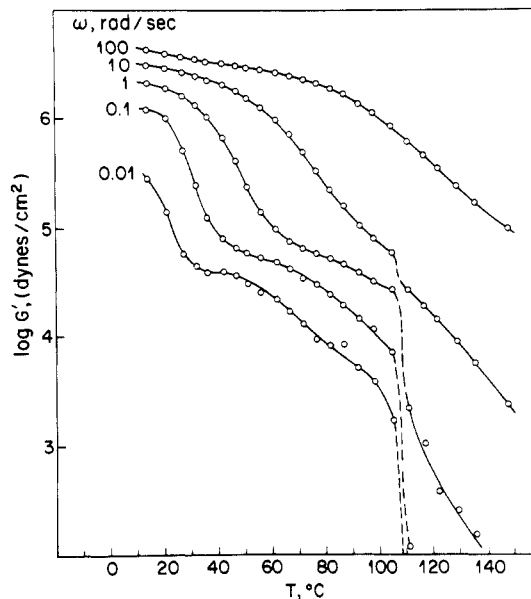


**Figure 3.** Dynamic elastic modulus obtained upon heating sample BB6. The discontinuity in  $G'$  at  $T_m = 108$  °C results from passing through the microphase separation transition. Below  $T_m$  the sample is in a microphase-separated (ordered) state while above  $T_m$  this polymer is homogeneous (disordered).

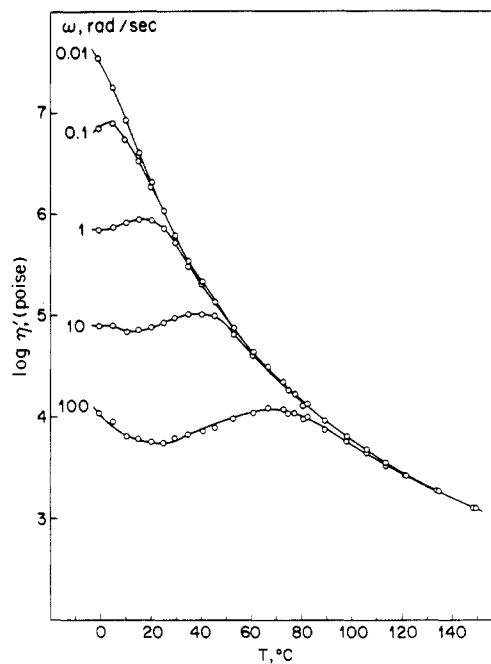


**Figure 4.** Dynamic viscosity of sample BB2. At low frequencies and high temperatures  $\eta'$  becomes Newtonian, characteristic of a homogeneous polymer liquid.

Figures 1–3 depict the elastic modulus vs. temperature over 5 decades of frequency for the three block copolymers. Measurements below  $10^2$  dyn/cm<sup>2</sup> were deemed unreliable based on the limitations set by the stress transducer of the RDS-7700 spectrometer. Figures 4–6 illustrate the dissipative characteristics of these materials over the same temperature range. In both sets of measurements, sample BB6 exhibits a discontinuity in modulus at low frequencies between  $105$  and  $111$  °C, which corresponds to the microphase separation transition. This result is discussed in detail in the following section.

Isothermal frequency scans were performed on each sample at various temperatures and are plotted in Figures 7–9. In each of these plots, the moduli have been corrected by  $T_r/T$  and frequency shifted to a reference tem-

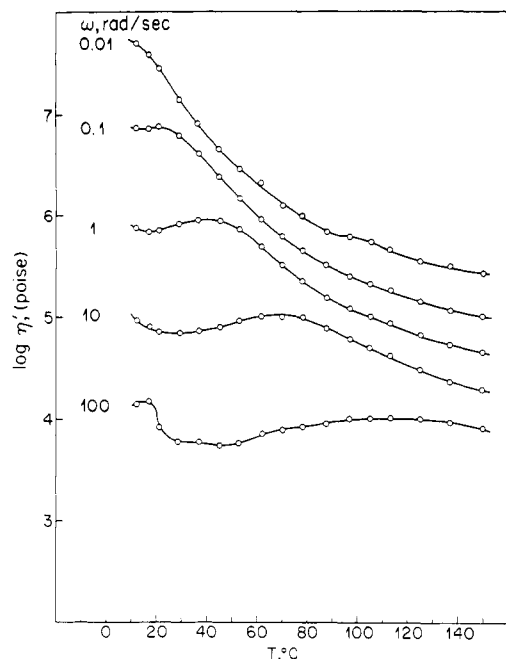


**Figure 5.** Dynamic viscosity of sample BB7. The highly non-Newtonian character of  $\eta'$  at low frequencies and high temperatures is a reflection of the ordered structure of this sample.

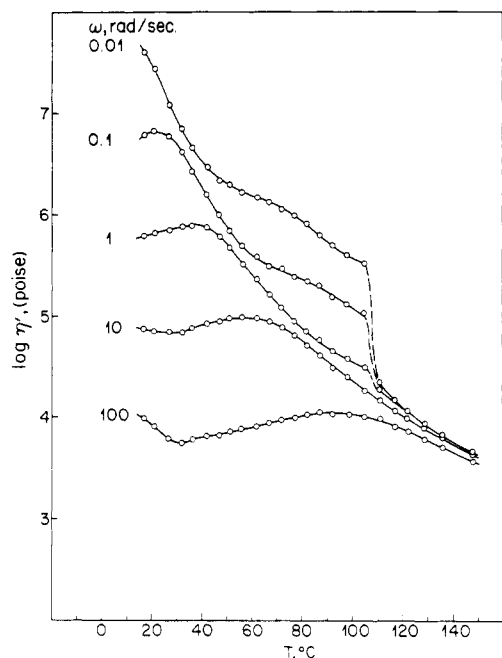


**Figure 6.** Dynamic viscosity obtained upon heating sample BB6. At  $T_m = 108^\circ\text{C}$ , this diblock copolymer undergoes a discontinuous change from a highly non-Newtonian to a nearly Newtonian form, which results from passing through the microphase separation transition.

perature,  $T_r$ , by an amount  $a_T$ .<sup>7</sup> The temperature dependence of these shift factors is plotted in Figure 10. These materials are, in fact, not rheologically simple, and as such the time-temperature superposition principle cannot be rigorously applied. Nevertheless, superpositioning the isothermal frequency scans is a very useful method of comparing and presenting these results. Emphasis in shifting has been placed on correlating the data in the plateau and initial part of the terminal region and assigning the peak in  $G''$ , between the plateau and terminal regions, to a constant reduced frequency. Below a critical reduced frequency the viscoelastic behavior of these materials can be quite complicated, as discussed below. Above this

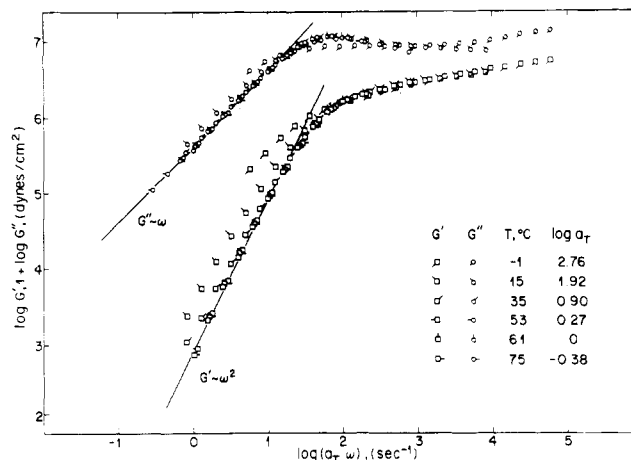


**Figure 7.** Reduced dynamic elastic and loss moduli for sample BB2. Lack of superposition at low reduced frequency and low temperature in this homogeneous polymer results from the presence of large composition fluctuations. The  $G''$  data have been shifted vertically 1 decade.

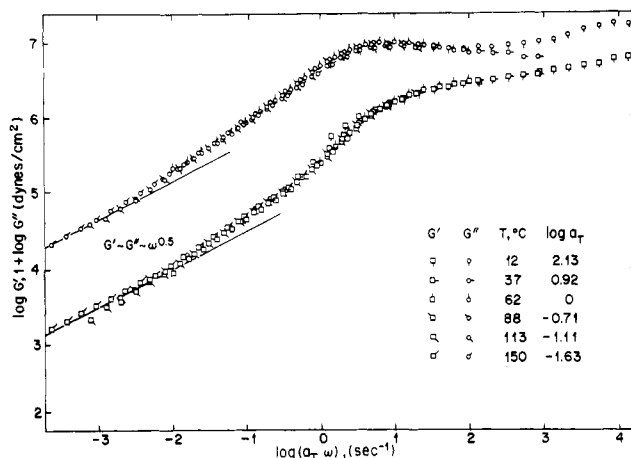


**Figure 8.** Reduced dynamic elastic and loss moduli for sample BB7. The  $G''$  data have been shifted vertically 1 decade.

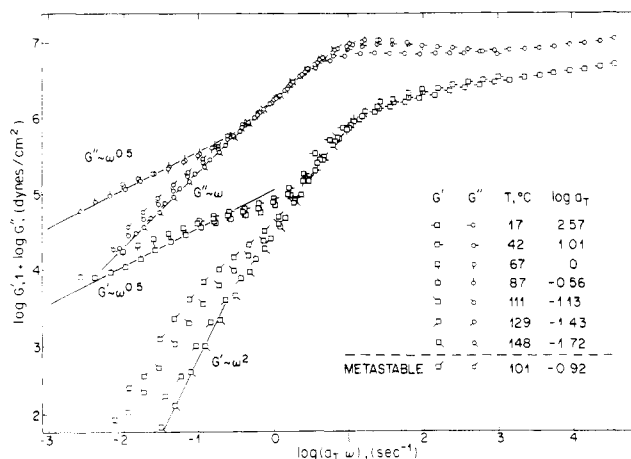


**Figure 9.** Reduced dynamic elastic and loss moduli for sample BB6. The two branches at low reduced frequency correspond to the microphase-separated and homogeneous states, above and below the melt transition temperature, respectively. The  $G''$  data have been shifted vertically 1 decade.

critical value the data shift satisfactorily.

The effects of thermal history on the discontinuity in the elastic modulus of sample BB6 was also investigated, and these results are presented in Figure 11. Just below  $111^\circ\text{C}$ , the low-frequency elastic modulus is strongly dependent on whether the sample has been heated or cooled,

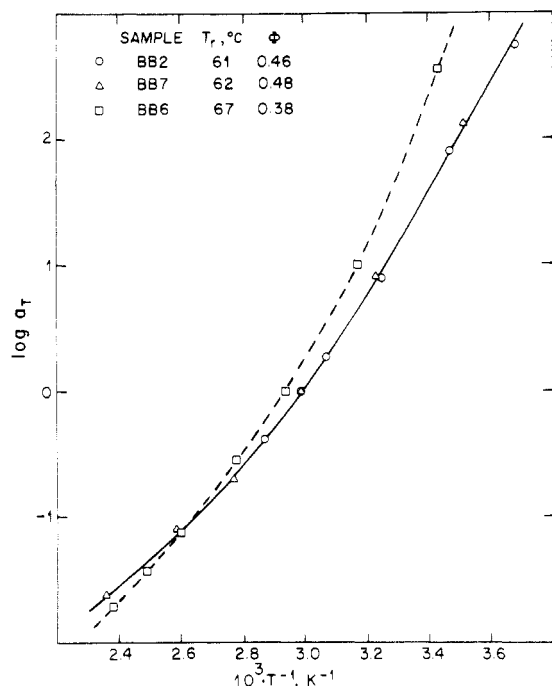


**Figure 10.** Comparison of the shift factors for the three diblock copolymers. Samples BB2 and BB7 are homogeneous and microphase separated, respectively, and sample BB6 undergoes a microphase separation transition at  $T_m^{-1} = 2.62 \times 10^{-3} \text{ K}^{-1}$ .

as discussed in the following section.

### Discussion

The results presented in Figures 1–11 provide a detailed picture of the structural behavior of block copolymers near

the microphase separation transition. Leibler<sup>1</sup> has calculated both the stability limit and equilibrium phase boundary, as well as the structure factor in the homogeneous melt, for block copolymers exhibiting upper critical temperature behavior. Samples BB2, BB6, and BB7 were designed to test these predictions through their necessary rheological implications. Concurrently, the detailed structure of the homogeneous melt has been examined by small-angle neutron scattering on a separate set of samples; these results are presented in separate reports.<sup>6</sup>

Intuitively, passing through the MST is expected to be accompanied by a dramatic change in viscoelastic properties, resulting from drastically different diffusion mechanisms in the disordered and ordered states. Diffusion in the homogeneous melt would be expected to proceed by the mechanism found in homopolymers (reptation), while the thermodynamic barrier imposed by microphase separation should eliminate (over experimentally accessible times) flow behavior above the MST. These results are a consequence of a coupling between the long-time relaxation processes and the structural order parameter in such one-component systems. In contrast, a simple binary mixture of homopolymers should exhibit no such rheological transitions upon phase separation.

The isochronal temperature scans presented in Figures 1–6 fully support these expectations. BB2, which remains below the MST over the experimental temperature range, rheologically resembles a homopolymer.<sup>7</sup> Increasing temperature and/or decreasing frequency brings about a transition from the plateau to the terminal zone in  $G'$  (Figure 1), while the dynamic viscosity proceeds from a frequency-dependent (non-Newtonian) to a frequency-independent (Newtonian) regime (Figure 4). For  $T \geq 53^\circ\text{C}$ , the low-frequency data ( $a_T\omega < 20$ ) presented in Figure 7

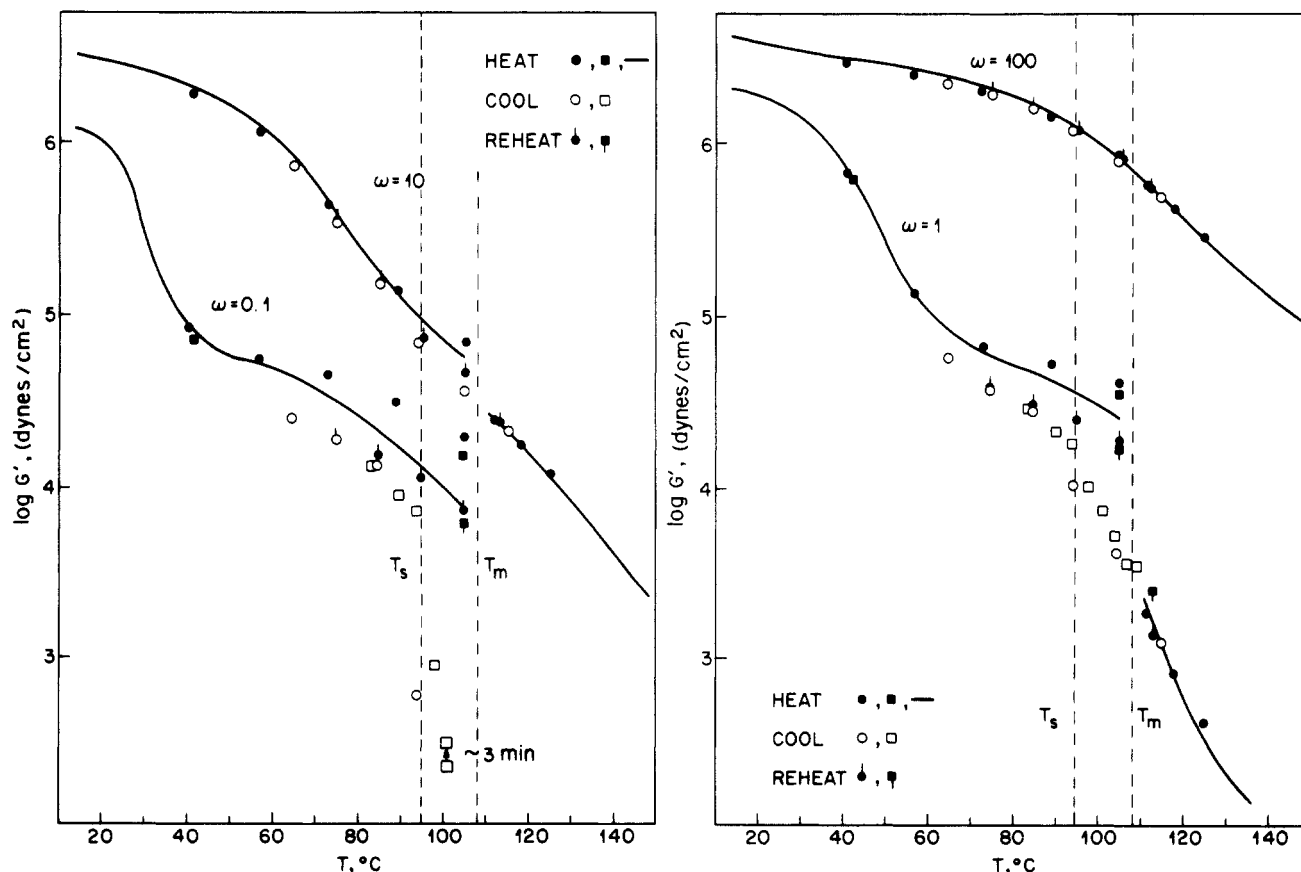


**Figure 11.** Effects of thermal history on the dynamic elastic modulus of sample BB6.  $T_m$  represents the experimentally determined MST temperature and  $T_s$  is the corresponding (calculated) spinodal temperature. The solid curves represent the data shown in Figure 3.

exhibit terminal-zone elastic and loss behavior;<sup>7</sup>  $G' \sim \omega^2$  and  $G'' \sim \omega$ . As the temperature is reduced below 53 °C, the frequency dependence of the elastic modulus begins to deviate from the terminal limit; at  $T = 15$  °C,  $G' \sim \omega^{1.7}$ . This latter effect derives from the development of composition fluctuations as discussed below. Overall, these results confirm that sample BB2 lies below the MST, in the homogeneous region of phase space.

In contrast to BB2, sample BB7 exhibits viscoelastic properties unlike those of homopolymer melts. At elevated temperatures and reduced frequencies, a second plateau in  $G'$  (Figure 2) and a highly non-Newtonian dynamic viscosity (Figure 5) characterize this material. Furthermore, the elastic and loss responses at low reduced frequencies (Figure 8) exhibit an apparent limiting behavior of  $G'' \sim G' \sim \omega^{0.5}$ . This dramatic change in viscoelastic properties upon increasing the degree of polymerization at constant composition results from passing through the MST; e.g., sample BB7 is microphase separated. Recall, the mean-field prediction for the phase boundary scales as the product  $\chi N$ , which is consistent with the phase behavior found in samples BB2 and BB7 (see Table I). With this understanding of the dynamic mechanical properties of 1,4-polybutadiene-1,2-polybutadiene diblock copolymers above and below the MST, the behavior of diblock copolymer on the phase boundary can be discussed.

As illustrated in Figure 11 and detailed below, the viscoelastic response of a block copolymer near the phase boundary can be strongly dependent on the thermal history of the sample. The initial discussion of the results obtained from sample BB6 will deal with data acquired while heating the polymer specimen; the effects of cooling are subsequently addressed.

The temperature dependence of the elastic modulus (Figure 3) and dynamic viscosity (Figure 6) obtained upon heating sample BB6 to 105 °C resembles that of BB7; there exists a secondary plateau in  $G'$  at low frequencies, and  $\eta'$  is highly non-Newtonian. Raising the temperature from 105 to 111 °C produces a discontinuous drop in both  $G'$  and  $\eta'$  at low frequencies. This discontinuity results from the melting of the ordered structure at the MST, where the melt temperature is given by  $T_m = 108 \pm 3$  °C. Above 108 °C the viscoelastic properties of BB6 are similar to those of BB2;  $G'$  approaches the terminal elastic limit, and  $\eta'$  is nearly Newtonian. These points are clearly illustrated in Figure 9. Above a critical reduced frequency  $((a_T\omega)_{c,G''} \simeq 0.3$  and  $(a_T\omega)_{c,G'} \simeq 3$  for sample BB6), the master curves of the three materials are nearly indistinguishable in form. For  $a_T\omega < (a_T\omega)_c$ , two branches are apparent in Figure 9, corresponding to data taken above and below  $T_m$ . The upper branches ( $T < T_m$ ) exhibit a limiting low-frequency character analogous to that found in BB7;  $G' \sim G'' \sim \omega^{0.5}$ . At the highest temperature, the low-frequency response approaches the terminal elastic limit; at  $T = 148$  °C,  $G' \sim \omega^2$  and  $G'' \sim \omega$ . Just above  $T_m$ , the lower branch in  $G'$  is distinctly nonterminal in character, intermediate in form to that at  $T = 148$  °C and  $T < T_m$ . The lower branches of  $G'$  and  $G''$  in Figure 9 (sample BB6) parallel the low reduced frequency results found in Figure 7 (sample BB2). This nonterminal elastic behavior at low  $a_T\omega$  is directly related to the structure of the homogeneous melt.

Leibler<sup>1</sup> has calculated the correlation function,  $S(Q)$ , which characterizes the homogeneous melt state in diblock copolymers

$$S(Q) = N / (F(Q; N, \Phi) - 2N\chi) \quad (1)$$

where  $F(Q)$  is a combination of Debye functions,  $Q = 4\pi\lambda^{-1} \sin(\theta/2)$  is the scattering wave vector, and  $\Phi = N_{1,4}/N$  is the composition. As  $F(Q)$  increases and approaches  $2N\chi$ ,

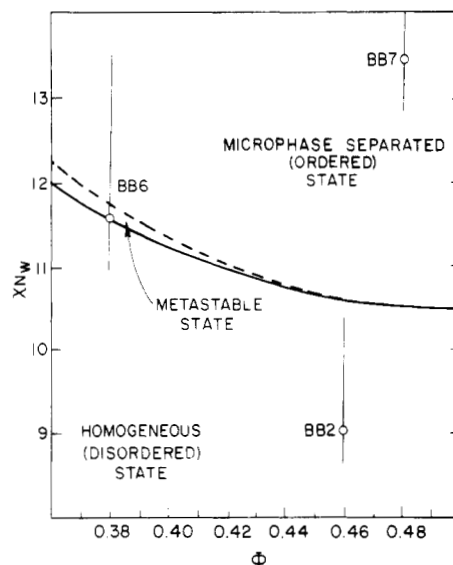


**Figure 12.** Predicted phase diagram for a diblock copolymer exhibiting upper critical temperature behavior. The points have been located based on  $T = 108$  °C, and the vertical lines indicate the estimated range in  $N\chi$  covered in the rheological experiments.

$S(Q)$  diverges. Near the critical composition ( $\Phi = 0.5$ ) this occurs around wave vector  $Q \simeq 2/R$ , where  $R$  is the overall radius of gyration of the block copolymer. This increase in  $S(Q)$  corresponds to the development of composition fluctuations of periodicity,  $D \simeq \pi R$ . The point of divergence,  $\chi N = (\chi N)_s$ , defines the stability limit. Taken over all compositions,  $(\chi N)_s$  establishes the spinodal curve. With the exception of the critical composition, the stability limit is preceded by a first-order phase transition, the MST;  $(\chi N)_{\text{MST}} < (\chi N)_s$ . At the critical composition, the phase transition becomes second order, and  $(\chi N)_{\text{MST}} = (\chi N)_s$ . Both the MST and spinodal limits, as determined by Leibler,<sup>1</sup> are plotted in Figure 12.

Equation 1 has been experimentally verified by this author as described in a separate report.<sup>6</sup> Quantitative agreement between the small-angle neutron scattering from a deuterium-labeled 1,4-polybutadiene-1,2-polybutadiene diblock copolymer (sample BB1,  $\Phi = 0.47$ ) and eq 1 was obtained with no adjustable parameters, where  $\chi$  was estimated from the rheological behavior of the presently discussed samples. Establishing the thermodynamic properties of block copolymers near the MST has provided the basis for interpreting the detailed viscoelastic behavior of samples BB6 and BB2.

Since  $\chi \sim T^{-1}$ , heating sample BB6 has the effect of reducing  $\chi N$ , driving this polymer toward the MST from the ordered state as shown in Figure 12. Under such conditions (heating the ordered material), the spinodal curve has no bearing on the structural or rheological properties of the sample. Passing through the MST results in a first-order phase transition, which produces the discontinuity in rheological properties found in Figures 3 and 6. At a composition corresponding to that of BB6,  $\Phi = 0.38$ , the MST is predicted to occur at  $(\chi N)_{\text{MST}} = 11.6$  (Figure 12). Therefore, based on  $N_w$ <sup>8</sup> (Table I), the interaction parameter at 108 °C is fixed at  $\chi = 8.2 \times 10^{-3}$ .

The previously quoted SANS study<sup>6a</sup> (of samples BB1 and BB3) demonstrated that  $\chi$  for this system cannot be assumed to be independent of composition. Setting  $\chi = 9.5 \times 10^{-3}$  produced excellent agreement between eq 1 and the scattering intensity from sample BB1 ( $\Phi = 0.47$ ) at 20 °C. Fitting eq 1 to the SANS results obtained from sample BB3 ( $\Phi = 0.18$ ) required a significant reduction in the interaction parameter. Over the presently considered

range of compositions,  $0.48 \leq \Phi \leq 0.38$ , variations in  $\chi$  appear to be considerably less significant. The small difference between the estimated value of  $\chi$  for BB6 at 108 °C and BB1 at 20 °C is consistent with the expected temperature dependence of the interaction parameter. Therefore, the locations in phase space corresponding to samples BB2, BB6, and BB7 have been assigned to Figure 12, with  $\chi = 8.2 \times 10^{-3}$  ( $T = 108$  °C). The range in  $\chi N$  corresponding to the temperature span covered in the dynamic mechanical measurements has been estimated by assuming<sup>9</sup>  $\chi = A + BT^{-1}$ , where the constants have been determined from the values of  $\chi$  measured at 20 and 108 °C by SANS and rheological measurements, respectively;  $A = 4.7 \times 10^{-3}$  and  $B = 1.35$ . A detailed SANS investigation of the temperature dependence of  $\chi$  for this set of polymers is in progress. Both the low-temperature behavior of sample BB2 (Figure 7) and the thermal history effects found in sample BB6 (Figure 11) can be accounted for based on Figure 12 and eq 1.

Above  $(\chi N)_{\text{MST}}$  the relaxation time of sample BB6 is shorter than the time required to achieve thermal stability and conduct an experiment. As a result, the measured elastic modulus over all frequencies is independent of the thermal history (Figure 11). Between  $(\chi N)_{\text{MST}} = 11.6$  and  $(\chi N)_s = 11.8$ , this sample is predicted to exist in a metastable state, where upon cooling, demixing should occur by nucleation, a slow, thermally activated process. This is confirmed by the viscoelastic behavior exhibited by sample BB6 upon cooling from 108 to 95 °C. Here, the measurement time is short relative to the time required for the sample to approach equilibrium. As a result, upon cooling, the low-frequency isochronal (Figure 11) and 101 °C isothermal  $G'$  data (Figure 9) appear to develop as continuations of the homogeneous melt state, as given by eq 1. A qualitative indication of the time-dependent nature of  $G'$  at  $T = 101$  °C is shown in Figure 11 for  $\omega = 0.1$ . A quantitative investigation of the time dependence of  $G'$  in the metastable state, which requires a complete knowledge of sample thermal history, will be undertaken in the future. Below the spinodal limit,  $\chi N < (\chi N)_s$ , the homogeneous melt state is unstable and should rapidly revert to the ordered state by a spinodal decomposition mechanism.<sup>10</sup> The low-frequency  $G'$  data of Figure 11 support this prediction. For  $T < 95$  °C the temperature dependence of  $G'$  in Figure 11 resembles that obtained upon heating. Here, thermal history effects on the elastic modulus are small and occur over much longer times (see below). In this case the measurement time is long relative to spinodal decomposition times.

The low-temperature, low reduced frequency behavior of sample BB2 (Figure 7) is analogous to the high-temperature ( $T_m < T < 150$  °C) results found in BB6. According to the estimate of  $N\chi(T)$ , the MST and spinodal limit should both occur at  $T_m \approx T_s \approx 0$  °C for  $\Phi = 0.46$ . Unfortunately, the data at this temperature do not extend sufficiently low in  $a_T\omega$  to confirm this prediction. Nevertheless, the magnitude of the deviations from the terminal elastic limit, which develop as the temperature is lowered, parallel the results from sample BB6 and indicate that  $T_s$  is close to 0 °C. As expected (Figure 12), sample BB7 remains microphase separated over the entire experimental temperature range.

There are also long-time changes in the level of the secondary plateau in  $G'$  for sample BB6. The data given by the filled symbols and listed under heating in Figure 12 were obtained from a specimen which had been aged at room temperature for several months. Results presented with a solid curve correspond to measurements taken 24

h after a specimen had been cooled to room temperature from 120 °C. The reheat data were obtained within 1 h of cooling below  $T_m$ . It is apparent that at low frequency, the secondary plateau in the elastic modulus, which is associated with the ordered structure, increases with time. According to Leibler,<sup>1</sup> just below  $T_m$  a body-centered-cubic ordered phase should develop in sample BB6, while at room temperature, the equilibrium phase symmetry is predicted to be hexagonal. Phase transformations of this type are expected to be extremely slow and may explain the long-time nature of the variations in this viscoelastic property.

The findings of this study corroborate those of previous reports<sup>2-4</sup> describing the dynamic mechanical properties of SBS and SIS triblock copolymer at elevated temperatures. Several unexplained differences between these investigations can also be resolved. Gouinlock and Porter<sup>3</sup> observed a sharp discontinuity in properties at approximately 142 °C, while Chung and Lin<sup>2</sup> found a narrow, but continuous, transition region between 140 and 150 °C. This difference was also reflected in the time-temperature superposition data. The former authors found that their low reduced frequency results shifted into two discrete branches, while the latter authors reported that data obtained in the transition region fell between these branches. Neither group provided any details concerning sample thermal history prior to measurement. Nevertheless, the results found in Figures 11 and 9 can account for these differences. Chung and Lin<sup>2</sup> also contradicted Gouinlock and Porter<sup>3</sup> in proposing that their shift factor vs. temperature data could be represented by two straight lines, above and below  $T_m$ . As illustrated in Figure 10, samples BB2 and BB7, which remain homogeneous and microphase separated, respectively, over the entire range of temperatures plotted, are characterized by a single shift factor curve.

Finally, it is interesting to note the apparent limiting low-frequency behavior of sample BB7 (and BB6 in the ordered state);  $G' \sim G'' \sim \omega^{0.5}$ . These samples might be expected to behave as a collection of tethered chains since one end of each block is thermodynamically restricted to the interfacial region between microdomains. According to the recent calculation of Pearson and Helfand<sup>11</sup> concerning star-shaped polymers, the predicted relaxation time for such chains is considerably shorter than that associated with the  $\omega^{0.5}$  dependence of the moduli in samples BB7 and BB6. Instead, this property must be associated with some other relaxation process, which may depend on microdomain geometry. The presently reported results cannot resolve this question since both ordered samples examined are predicted to contain a lamellar morphology.<sup>12</sup>

## Conclusions

This second in a series of articles concerning block copolymers near the microphase separation transition (MST) has focused on examining the linear dynamic mechanical properties of a model set of diblock copolymers. Owing to the connectivity between chemically dissimilar blocks, the order-to-disorder transition in block copolymers is accompanied by a dramatic change in the low-frequency shear moduli, which provides a unique opportunity for studying the thermodynamics of polymer-polymer miscibility. In this manner, both the microphase separation transition and spinodal curve have been identified in the system consisting of 1,4-polybutadiene-1,2-polybutadiene diblock copolymers; such information cannot be obtained from the rheology of homopolymer blends. These results, in conjunction with the small-angle neutron scattering

(SANS) study reported separately<sup>6a</sup> and to be presented as the third installment of this series,<sup>6b</sup> quantitatively confirm the mean-field predictions of Leibler<sup>1</sup> concerning the structure and phase behavior of block copolymers. This study has demonstrated that the rheological analysis of block copolymers represents a powerful method of investigating polymer-polymer thermodynamics.

**Acknowledgment.** I am grateful to V. Reddy Raju for helpful discussions and for his assistance in using the mechanical spectrometer and to Mark A. Hartney for his collaboration in preparing the samples.

## References and Notes

- (1) Leibler, L. *Macromolecules* **1980**, *13*, 1602.
- (2) Chung, C. I.; Lin, M. I. *J. Polym. Sci., Polym. Phys. Ed.* **1978**, *16*, 545; Chung, C. I.; Gale, J. C. *J. Polym. Sci., Polym. Phys. Ed.* **1976**, *14*, 1149.
- (3) Gouinlock, E.; Porter, R. *Polym. Eng. Sci.* **1977**, *17*, 534.
- (4) Widmaier, J. M.; Meyer, G. C. *J. Polym. Sci. Polym. Phys. Ed.* **1980**, *18*, 2217.
- (5) Bates, F. S.; Bair, H. E.; Hartney, M. A. *Macromolecules* **1984**, *17*, 1987.
- (6) (a) Bates, F. S. *Macromolecules*, in press. (b) Bates, F. S.; Hartney, M. A., to be submitted to *Macromolecules*.
- (7) Ferry, J. D. "Viscoelastic Properties of Polymers", 2nd ed.; Wiley: New York, 1970.
- (8) de Gennes, P.-G. "Scaling Concepts in Polymer Physics"; Cornell University Press: Ithaca, NY, 1979.
- (9) Roe, R.-J.; Zin, W.-C. *Macromolecules* **1980**, *13*, 1221.
- (10) Cahn, J. W. *Trans. Metallurg. Soc. AIME* **1968**, *242*, 166.
- (11) Pearson, D. S.; Helfand, E. *Macromolecules* **1984**, *17*, 888.
- (12) Helfand, E.; Wasserman, Z. R. In "Developments in Block Copolymers"; Goodman, I., Ed.; Applied Science Publishers: London, 1982.

## Simultaneous Curing and Filling of Elastomers

James E. Mark,\* Cheng-Yong Jiang,<sup>†</sup> and Ming-Yang Tang<sup>†</sup>

Department of Chemistry and the Polymer Research Center, The University of Cincinnati, Cincinnati, Ohio 45221. Received February 15, 1984

**ABSTRACT:** A method previously developed for the precipitation of reinforcing silica filler within an already cured elastomer is extended so as to permit simultaneous curing and filling. Specifically, tetraethyl orthosilicate is used to end-link hydroxyl-terminated chains of poly(dimethylsiloxane), with the excess present being hydrolyzed to finely divided SiO<sub>2</sub>. Increase in the amount of filler thus formed decreases the elongation required for the desired upturns in modulus and increases the maximum extensibility, ultimate strength, and energy required for rupture of the network.

## Introduction

Elastomers which cannot readily undergo strain-induced crystallization are very weak in the unfilled state.<sup>1-3</sup> Networks of poly(dimethylsiloxane) (PDMS) [-Si(CH<sub>3</sub>)<sub>2</sub>-O-] are in this category, primarily because of the very low melting point (-40 °C)<sup>4</sup> of this polymer. As a result, PDMS elastomers used in most applications are invariably filled with a "high-structure" particulate silica (SiO<sub>2</sub>) in order to improve their mechanical properties.<sup>5-8</sup> The incorporation of such fillers in PDMS or any high-viscosity polymer, however, is a difficult, time-consuming, and energy-intensive process.<sup>5-8</sup> It can also cause premature gelation ("structuring" or "crepe hardening").<sup>9</sup> For these and other reasons,<sup>10</sup> it would be advantageous to be able either to precipitate reinforcing SiO<sub>2</sub> into an already cured network or to generate it during the curing process. The first goal was achieved in two earlier studies<sup>10,11</sup> in which tetraethyl orthosilicate (TEOS) [Si(OC<sub>2</sub>H<sub>5</sub>)<sub>4</sub>] was hydrolyzed to precipitate the desired SiO<sub>2</sub> filler into a cross-linked PDMS network. The present investigation extends this work so as to permit the simultaneous curing and filling of an elastomer material.

## Experimental Details

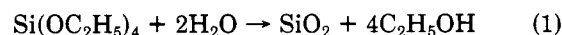
The polymers employed, two hydroxyl-terminated PDMS samples having number-average molecular weights corresponding to 10<sup>-3</sup>M<sub>n</sub> = 21.3 and 8.00, respectively, were generously provided by Dow Corning Corp. Portions of them were mixed with TEOS in amounts characterized by the molar feed ratio  $r = [\text{OC}_2\text{H}_5]/[\text{OH}]$ , where the OC<sub>2</sub>H<sub>5</sub> groups are on the TEOS and

the OH groups appear as chain ends on the PDMS. Specific values of this ratio, which range upward from 1.0 (stoichiometric balance), are given in the third column of Table I. The catalysts employed, dibutyltin diacetate and stannous 2-ethyl hexanoate, were present to 0.8-1.0 and 1.7 wt %, respectively, of the PDMS. Both series of mixtures of these three components appeared to be perfectly homogeneous. They were poured into molds to a depth of 1.0-1.5 mm, and the reaction was allowed to proceed at room temperature for 3 days. The water required for the hydrolysis of the TEOS was generally simply absorbed from the humidity in the air,<sup>12</sup> but in a few test cases, additional liquid water was added to the reaction media.

The resulting networks were extracted in tetrahydrofuran and toluene in the usual manner;<sup>13,14</sup> the sol fractions thus obtained are small, as can be seen from the values given in column four of Table I. The densities  $\rho$  of these extracted materials were determined by pycnometry. Swelling measurements in benzene at room temperature were also carried out on portions of the extracted samples. Similarly, other unswollen portions were used in the elongation experiments carried out to obtain the stress-strain isotherms at 25 °C.<sup>13,14</sup> The nominal stress was given by  $f^* \equiv f/A^*$ , where  $f$  is the elastic force and  $A^*$  the undeformed cross-sectional area, and the reduced stress or modulus<sup>1,13-15</sup> by  $[f^*] \equiv f^*/(\alpha - \alpha^{-2})$ , where  $\alpha = L/L_i$  is the elongation or relative length of the sample.

## Results and Discussion

The simplest equation for the hydrolysis of TEOS is



but the reaction in the presence of the hydroxyl-terminated PDMS is probably much more complicated, with some chains bonded to incompletely hydrolyzed products. In any case, electron microscopy results<sup>16</sup> indicate the particles to be unagglomerated, with an average diameter of

<sup>†</sup> Visiting scholar from the Chenguang Institute of Chemical Industry, Sichuan, China.